VERA Geodetic VLBI with a Newly Developed High-speed Sampler and Recorder

Takaaki Jike

Abstract By using 1-Gbps recording and increasing the number of scans, VERA has improved the accuracy of the parameter estimation in geodetic VLBI, guaranteeing accurate VERA astrometry. However, further increasing the number of scans will be difficult given the slew speeds of the VERA antennas. OCTAD and OCTADISK2 are candidates for the next-generation data processing system of VERA. The sampling/recording rate of the new system is 8 Gbps. The broadening of the recording bandwidth leads to an improved delay estimation accuracy and is expected to improve the accuracy of the geodetic results. We performed several geodetic VLBI experiments using the new high-speed sampler and recorder.

Keywords VERA, 8-Gbps sampler

1 Introduction

VERA is a Japanese VLBI array aimed for obtaining a three-dimensional map of our Galaxy. Four antennas (Mizusawa, Iriki, Ogasawara, and Ishigakijima) form the VERA network. Employing a phase-referencing VLBI technique, VERA will measure distances and motions of radio sources in our Galaxy with an accuracy of 10^{-9}, unveiling the true structure of our Galaxy. In order to guarantee the accuracy of VERA astrometry, VERA is carrying out two kinds of geodetic VLBI observations. One is the participation of VERA-Mizusawa in IVS sessions (T2, AOV) tying the VERA network into the TRF. The other is VERA-internal geodetic VLBI in K-band for monitoring the VERA network at the mm-level (H: 1 mm, V: 3–4 mm). The current observation specifications of the VERA-internal geodetic VLBI are shown in Table 1.

National Astronomical Observatory of Japan

Table 1 Specifications of the current VERA-internal geodetic VLBI in K-band.

Number of scans	500–800
Sampling mode	1024Mbps-2bit-1ch
Digital filter mode	16MHz-2bit-16ch, 32-MHz interval
Received radio frequency	22,800–23,328 MHz
Data storage system	OCTADISK
Recording rate	1024 Mbps
Correlator	Mizusawa GICO3

From the site positions derived from the VERA-internal geodetic VLBI observations, the following features are discernible. The largest feature for all stations except Mizusawa is a linear change in position caused by plate motion. For Mizusawa, a co-seismic step and post-seismic creeping are predominant. With the other stations, velocity changes from slow-slip-events (SSE) can be seen. They exert fluctuations from several millimeters to several centimeters on the site positions, and it is difficult to predict the time of the SSE event and the size of the fluctuations. Typical errors for the position results are 1 mm in horizontal and 4 mm in the vertical, but the variation between the results is about twice the size of the errors.

Is it possible to improve the reliability of the estimated site coordinates to 2–3 mm? One of the approaches for improving the accuracy of the estimated geodetic parameters is the acquisition of more precisely and more accurately observed delays. The desired accuracy for the estimated delays is a few millimeters in length (less than 10 ps, 5–6 ps on average).

Broadening the recording bandwidth is effective to the improve the fringe detection sensitivity and the accuracy of the estimated delay. OCTAD and OCTADISK2 of the OCTAVE series [1] are a newly developed high-speed sampler and recorder, respectively, developed by NAOJ. The specifications of OCTAD are given in Table 2. Experimental geodetic VLBI observations were carried out using the high-speed sampler and recorder in order to confirm the improvement in the accuracy of the geodetic estimation parameters by the broadening of the recording bandwidth.

Table 2 Specifications of OCTAD.

Maximum sampling rate	10,384 Mbps
Quantifying bit number	2 or 3 bit
Output	10GbE
10GbE ch. number	4 in maximum
10GbE application layer protocol	VDIF

2 Selection of Radio Sources

It is required that the effect of the radio source structure on the uncertainty of the delay amounts to less than 10 ps. Hence, radio sources with a median value for the delay correction due to source structure of less than 10 ps become candidates for observation. In practical terms, radio sources with a structure index of less than two are chosen from the list of K/Q band sources [2]. Each source in this list may or may not have a successful fringe detection. A judgment is performed under the following conditions: delays are estimated with an error of 10 ps or less, each radio source is observed simultaneously at all VERA sites, and fringes are detected with an integration time of 120 seconds or less. Table 3 summarizes the prediction results using three sampling/recording modes: VERA's currently used 1-Gbps mode, 2-Gbps as the maximum performance of the currently used sampler at VERA, and 8-Gbps as the highest possible bit rate. Accordingly, in order to realize geodetic VLBI observations with a delay accuracy of 10 ps or better, the sampling/recording rate of 8-Gbps is indispensable.

Table 3 Predicted performance of the fringe detection.

Sampling mode (MHz-bit)	512-2	1024-2	4096-2
Minimum SNR	280	65	45
Minimum flux density (Jy)	4.54	0.80	0.28
Number of sources with fringes	0	8	170

3 Observation

Details of the geodetic VLBI experiment are shown in Table 4. Three recording modes were used during the experiment: 1-Gbps, 2-Gbps, and 8-Gbps; their respective parameters to achieve the needed accuracy change in the geodetic parameter estimation with a broadened recording bandwidth are listed in Table 5. Although the observation period was originally planned to be 24 hours, the actual observing time length became 13 hours because of a data transfer problem in the middle of the observation period.

Table 4 Details of the geodetic VLBI experiment.

Date	06:00 Jan. 27 – 06:06 Jan. 28, 2016
Baseline and length	Mizusawa–Ishigakijima, 2280 km
Sky condition	fine@Mizusawa, rain@Ishigakijima
Predicted minimum SNR	38
Number of usable scans	255

Table 5 Comparison of the three data acquisition systems.

Mode name	1-Gbps	2-Gbps	8-Gbps
Sampler	ADS1000	ADS3000+	OCTAD
Filter (MHzBW-bit-ch)	16-2-16	512-2-1	512-2-4
Recorder	OCTADISK	VSREC	OCTADISK2
Min. freq. (MHz)	22,700	21,971	21,459
Rec. rate (Mbps)	1024	2048	8196
Effective BW (MHz)	147.51	147.80	591.21

4 Results of Delay Estimation

Table 6 shows the estimation results of the delays acquired with the three sampling modes. These delays were estimated using the same scan observing radio source 0016+731 for 40 seconds. The estimated delay error is a few ps for 8-Gbps. Table 7 lists the average SNR ratios for 8-Gbps/1-Gbps and 2-Gbps/1-

Table 6 Results of the delay estimation.

Rec. Rate	Delay Error (ps)	SNR
1-Gbps	18.8	57.1
2-Gbps	10.7	100.2
8-Gbps	1.2	219.3

Table 7 Theoretical and actual SNR ratios.

	2-Gbps/1-Gbps	8-Gbps/1-Gbps
Theoretical SNR ratio	1.45	2.88
Average SNR ratio	1.77	3.72

Gbps as determined from the delay estimation. Hence, the actual measured ratio is larger than the theoretical one. This result suggests that the coherence loss occurring in the 1-Gbps signal transfer system is larger than the ideal value. The standard deviation (S.D.) of the delay differences were 30.44 ps between 8-Gbps and 2-Gbps and 74.40 ps between 2-Gbps and 1-Gbps, respectively. The scatter of the delay decreased when the recording bandwidth was broadened and/or the SNR was increased.

5 Results of Rapid Geodetic Estimation

The antenna coordinates, clock polynomials, and zenith atmospheric delay correction parameters (dZAD) were estimated simultaneously. Table 8 shows the offsets and errors of the antenna coordinates as estimated from observations in each sampling mode. The distribution of the error ellipsoids is shown in Figure 1. The offsets from the initial coordinates are settled in less than several millimeters. The ratio of the magnitude of the error for 1-Gbps:2-Gbps:8-Gbps is 2.0:1.4:1.0.

Table 8 Estimated offsets and errors of the Ishigakijima antenna coordinates (in mm).

	1-Gbps		2-Gbps		8-Gbps	
	offset	error	offset	error	offset	error
U–D	2.1	7.0	−5.3	5.2	2.6	3.4
E–W	1.5	2.0	1.4	1.7	−2.3	1.1
N–S	1.0	2.3	−0.4	1.6	−0.8	1.1

The estimated errors are shown in Table 9. For the 1-Gbps and 2-Gbps modes, the RMS of the post-fit delay residuals and the RMS of the observed delay errors are close in value. This suggests that the magnitude of the errors of the estimation parameters is dependent on the magnitude of the thermal noise error of the observed delay. However, with 8-Gbps, the RMS of the post-fit delay residuals is 4.2 times larger than the RMS of the observed delay error. Thus, the ability of the delay estimation is not used effectively in the analysis. Possible reasons for this could be: the instability of the observation system, a time variation of the inter-band phase characteristics, unsuitableness of the fitting function of the fringe peak search processing, skewness of the delay resolution function, and insufficient precision of the physical model and observation equation.

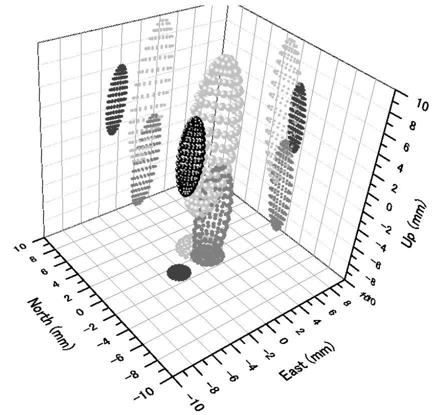

Fig. 1 Distribution of the error ellipsoids from the initial coordinates. The smallest ellipsoids show the error distribution for 8-Gbps, the medium-sized for 2-Gbps, and the largest for 1-Gbps.

A misestimation of dZAD and its time variation exerts large uncertainties on the estimated coordinates. It is confirmed that the estimation ability of dZAD can be improved by reducing the delay estimate errors. Figure 2 depicts the time series of the estimated dZAD obtained from 1-Gbps, 2-Gbps, and 8-Gbps, respectively. Table 10 lists the average value of the estimated dZAD and its standard deviation. It can be seen that the error scale and time variation of dZAD decreases with decreasing observed delay errors. The error of the estimated dZAD is about six times larger than the RMS of the observed delay error in 8-Gbps. If the atmospheric propagation delay model can trace delays with higher accuracy, it is likely that the estimation of the dZADs will become more exact. Also, it will be effective to go to a higher scanning frequency to estimate dZAD. It is necessary to confirm that a stabilization of the dZAD

Table 9 Estimation errors.

Mode Name	1-Gbps	2-Gbps	8-Gbps	2-Gbps/1-Gbps	8-Gbps/1-Gbps
RMS of post-fit residuals [ps]	32.2	23.0	14.0	0.71	0.43
Sample standard deviation [ps]	2.4	1.7	1.0	0.70	0.42
Degrees of freedom	177	185	186		
Error of baseline length [mm]	8.6	6.0	4.1	0.69	0.48
RMS of observed delay error [ps]	34.7	21.0	3.3	0.61	0.10
Delay rejection criterion [ps]	159.6	115.3	71.5		

results contributes to the stability of the antenna coordinates results.

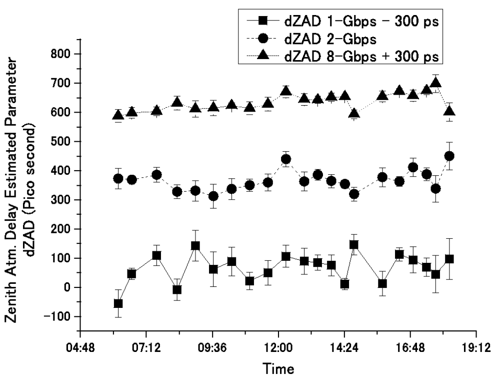

Fig. 2 Time series of the estimated zenith atmospheric delay correction. The mapping function used in the estimation was NMF.

Table 10 Average and standard deviation of the estimated dZAD parameters (in ps).

Mode	Average	Std. Dev.
1-Gbps	367.17	38.25
2-Gbps	366.89	26.86
8-Gbps	334.20	18.73

6 Conclusions

A geodetic VLBI experiment was carried out with three data processing systems in order to confirm an improvement in the accuracy of the geodetic estimation parameters by broadening the recording bandwidth. The employed sampling/recording modes were 1-Gbps, 2-Gbps, and 8-Gbps. When compared to 1-Gbps recording, the SNR of the fringes increased 1.5-fold for 2-Gbps and 3.5-fold for 8-Gbps. The RMS of the observed delay error reached 3 ps for 8-Gbps, thanks to a widening of the recording bandwidth. The delay scatter was also reduced. The magnitude ratio of the geodetic solution error is 2.0, 1.4, and 1.0 for 1-Gbps, 2-Gbps, and 8-Gbps, respectively. The time series stability of the zenith atmospheric delay correction also improved.

Future goals are to perform test observations with 800 or more scans per 24 hours, repeating test observations in order to confirm the stability of the estimated antenna coordinates, establishment of regular operation with 8-Gbps recording, and the use of OCTAD for international VLBI observations at VERA-Mizusawa.

References

1. Y. Kono, T. Oyama, N. Kawaguchi, S. Suzuki, K. Fujisawa, H. Takaba, K. Sorai, M. Sekido, S. Kurihara, Y. Murata, H. Uose, “Real-time VLBI Network with 10GbE Connection, OCTAVE”, In D. Behrend and K. Baver, editors, *International VLBI Service for Geodesy and Astrometry 2012 General Meeting Proceedings*, NASA/CP-2012-217504, pages 96–98, 2012.
2. P. Charlot, D. A. Boboltz, A. L. Fey, E. B. Fomalont, B. J. Geldzahler, D. Gordon, C. B. Jacobs, G. E. L. Lanyi, C. Ma, C. J. Naudet, J. D. Romney, O. J. Sovers, and L. D. Zhang, “The Celestial Reference Frame at 24 and 43 GHz. II. Imaging”, *The Astronomical Journal*, 139, pages 1713–1770, doi:10.1088/0004-6256/139/5/1713, 2010.